Identification of novel Prominin-1/CD133 splice variants with alternative C-termini and their expression in epididymis and testis

Christine A. Fargeas[1], Angret Joester[1], Ewa Missol-Kolka[1], Andrea Hellwig[2], Wieland B. Huttner[1,*] and Denis Corbeil[1,3,*]

[1]Max-Planck-Institute of Molecular Cell Biology and Genetics, Pfotenhauerstrasse 108, 01307 Dresden, Germany
[2]Department of Neurobiology, University of Heidelberg, Im Neuenheimer Feld 364, 69120 Heidelberg, Germany
[3]Medical Clinic and Polyclinic I, Technical University Dresden, Fetscherstrasse 74, 01307 Dresden, Germany
*Authors for correspondence (e-mail: huttner@mpi-cbg.de; corbeil@mpi-cbg.de)

Accepted 11 May 2004
Journal of Cell Science 117, 4301-4311 Published by The Company of Biologists 2004
doi:10.1242/jcs.01315

Summary

Prominin-1/CD133 is a five-membrane-span glycoprotein that is thought to act as an organizer of plasma-membrane protrusions. Here, we report the molecular and cell-biological characterization of four novel prominin-1 splice variants isolated from a mouse testis cDNA library and referred to as prominin-1.s3 to prominin-1.s6. Compared with kidney-derived prominin-1.s1, the s3, s4 and s5 variants contain a distinct cytoplasmic C-terminal domain. The s4 and s5 variants bear, in addition, two and one in-frame deletion(s), respectively, in the extracellular domains. The s6 variant displays a truncated C-terminal domain caused by a premature termination resulting from intron retention. Upon their ectopic expression in Chinese hamster ovary cells, the s3 and s6 variants were found to be concentrated in plasma-membrane protrusions, whereas the s4 and s5 variants did not reach the cell surface. Biochemical analyses suggest that most of the prominin-1 in the adult male reproductive system is expressed as the s6 variant. Immunohistological and electron microscopic analyses show that prominin-1 is: (1) confined to the apical surface of the epithelium all along the epididymal duct, with the exception of the initial segment; (2) concentrated in stereocilia of the epididymal duct epithelium; and (3) found on the tail of developing spermatozoa in seminiferous tubules. Our data suggest that prominin-1 is involved in the formation and/or stabilization of epididymal stereocilia and the tail of spermatozoa, and hence might play a dual role in the biogenesis of spermatozoa.

Supplemental data available online

Key words: Prominin-1, CD133, Microvilli, Epididymis, Spermatozoa

Introduction

Prominin-1/CD133 is the first characterized member of an emerging family of multispan membrane proteins that display a unique structure, with five transmembrane segments and two large glycosylated extracellular loops (Weigmann et al., 1997; Fargeas et al., 2003a; Fargeas et al., 2003b) (for review, see Corbeil et al., 2001b). Prominin-1 is widely distributed throughout the animal kingdom. In addition to the rodent (Weigmann et al., 1997; Corbeil et al., 2001a) and human (Miraglia et al., 1997) prominin-1, predicted prominin-like molecules have been identified in worm, fly, fish and chicken (Weigmann et al., 1997; Corbeil et al., 1998; Fargeas et al., 2003a). In mammals, prominin-1 is expressed in various embryonic and adult epithelial cells (Weigmann et al., 1997; Corbeil et al., 2000; M. Florek, M. Haase, A.-M. Marzesco, D. Freund, G. Ehninger, W.B.H. and D.C., unpublished data) as well as in non-epithelial cells, notably rod photoreceptor cells (Maw et al., 2000). Prominin-1 appears to be a useful novel cell surface marker to identify and isolate stem cells from various sources including the hematopoietic and central nervous system (Yin et al., 1997; Uchida et al., 2000) (for review, see Bhatia, 2001).

Prominin-1 displays a remarkable subcellular localization. At the plasma membrane, prominin-1 is confined to specific subdomains that, although distinct in various cell types, have one feature in common – they protrude from the planar region of the plasmalemma. In epithelial cells, prominin-1 is concentrated in microvilli and similar protrusions of the apical plasma membrane, and is lacking from the planar subdomain of the cell surface (Weigmann et al., 1997; Corbeil et al., 1999; Corbeil et al., 2000). In non-epithelial cells, such as hematopoietic stem cells, prominin-1 is again enriched in plasma-membrane protrusions (Corbeil et al., 2000). In rod photoreceptor cells, prominin-1 is concentrated in the plasma-membrane evaginations present at the base of the outer segment (Maw et al., 2000), which are essential precursor structures in the biogenesis of photoreceptive disks (Steinberg et al., 1980).

We have showed that the specific localization of prominin-1 in plasma-membrane protrusions of epithelial cells involves a novel membrane microdomain in which prominin-1 interacts specifically with cholesterol (Röper et al., 2000). Although no function has yet been ascribed to prominin-1, the general preference of this membrane protein for plasma-membrane

protrusions and the identification of a frame-shift mutation in the human *PROMININ-1* gene that prevents its cell-surface appearance and causes retinal degeneration (Maw et al., 2000) have led to the hypothesis that prominin-1 acts as an organizer of plasma-membrane protrusions (Corbeil et al., 2001b). For example, prominin-1 might endow plasma-membrane protrusions with an appropriate lipid composition, particularly with respect to cholesterol. The observation that, in rods, the newly synthesized photoreceptive disks are enriched in cholesterol (Boesze-Battaglia et al., 1989) is consistent with this hypothesis.

The *PROMININ-1* gene is known to consist of at least 27 exons (Maw et al., 2000; Yu et al., 2002; Fargeas et al., 2003a). To obtain further clues about the physiological function of prominin-1, it is important to investigate the possibly tissue-specific alternative splicing of prominin-1, given that this protein is expressed in many different epithelial and non-epithelial cells, and is associated with various types of plasma-membrane protrusions (Corbeil et al., 2001b). In the present study, we report the identification of novel prominin-1 splice variants with alternative cytoplasmic C-termini, and their cell biological characterization in the male reproductive system. In agreement with the postulated function of prominin-1 as an organizer of plasma-membrane protrusions, the presence of specific splice variants of prominin-1 in stereocilia of epididymal epithelia and in the flagellate tail of developing spermatozoa (when present in seminiferous tubules) suggests that prominin-1 might play a role in the morphogenesis of these protrusions.

Materials and Methods

Identification and molecular cloning of prominin-1 splice variants

Nucleotide and protein databases were searched at the National Center for Biotechnology Information using the BLAST network services. A TblastN search on the dbEST database using the mouse prominin-1 protein sequence (GenBank accession number AF026269) as a probe retrieved one mouse testis expressed sequence tag (EST) clone (GenBank accession number AV273635) listed as similar to the human genomic clone containing the *PROMININ-1* gene (GenBank accession number AC005598). The EST clone 4932412G18 aligned from nucleotides 1-134 with murine prominin-1 cDNA sequence 2523-2656 (94% identity) and showed from nucleotides 154-176 100% identity with the intronic sequence of human *PROMININ-1* gene. Because nucleotide position 134 corresponds to the boundary of exons 23 and 24 of human *PROMININ-1* gene, this EST clone could represent a splice variant of prominin-1. Oligonucleotide primers were designed to amplify this potential splice variant from a mouse testis cDNA pool using the polymerase chain reaction (PCR). A 5′ sense primer (5′-TACCAGCCAGGAGGCAGAAGAG-3′) corresponding to the sequence 90-111 of the prominin-1 cDNA (GenBank accession number AF026269) was used together with a 3′ antisense primer (AS-T1; 5′-CATGCATGTTCACCAGACACAGAAC-3′) corresponding to position 216-240 of the EST clone 4932412G18 in a PCR reaction using first-strand cDNA from mouse testis poly $(A)^+$ RNA (Clontech; catalog number K1423-1) as template. The PCR reaction, performed using Advantage® cDNA Polymerase Mix (Clontech) according to the manufacturer's instructions, generated a fragment of about 2.5 kb. An aliquot of the PCR product was purified and subcloned in the pCR®-Blunt II TOPO vector according to the manufacturer's instructions (Zero Blunt™ TOPO™ PCR cloning kit; Invitrogen, Groningen, The Netherlands). cDNA inserts were completely sequenced on both strands using the Autoread™ sequencing kit and an ALFexpress™ sequencer (Amersham Pharmacia Biotech, Freiburg, Germany).

3′-RACE (rapid amplification of DNA ends) was carried out on mouse 11-day whole-embryo Marathon Ready cDNA (Clontech; catalog number 7458-1) according to the manufacturer's instructions. The first PCR reaction was performed using gene-specific sense primer (5′-GGACCCTCCAGCAAACAAGCAAC-3′; nucleotides 2266-2288 of GenBank accession number AF026269), which is specific for the sequence encoding a part of the second extracellular loop of prominin-1, and the linker-specific adaptor primer 1 supplied with the Marathon Ready cDNA kit. The nested gene-specific sense primers NS-TA (5′-ACTCGTCCGTCTCGGGGATGTG-3′) or NS-TB (5′-GATAACTTGTCGTTGCTCCTTCC-3′) matching nucleotides 2567-2588 and 2603-2625, respectively, of one of the prominin-1 splice variants obtained above (GenBank accession number AF305215) were used with the linker-specific adaptor primer 2 for the second PCR reaction. The nested PCR products were subcloned in the pCR-Blunt II TOPO vector and sequenced as above.

Northern-blot analysis

Northern-blot analyses were performed using mouse multiple-tissue northern-blot membrane (Clontech, catalog number 7762-1). The *Bam*HI-*Bam*HI prominin-1 cDNA fragment (nucleotides 735-1466) released from the bacterial expression plasmid pGEX-E2 (Corbeil et al., 1999) and the prominin-1 PCR product (nucleotides 2793-3599) were used to generate the prominin-1-specific cDNA probes E2 and 3′-UTR, respectively. For the selective PCR amplification of the 3′-UTR probe, the sense (5′-CAAGATAGTCAACATG-GAAAGCATCACAG-3′) and antisense (5′-GACCAGAT-GACACTGAACGTAATGCC-3′) primers were used together with the pCR-TOPO 3′-UTR-B10 plasmid as template. Probes were labeled with [α-^{32}P]dCTP by the random-prime method using the Rediprime kit (Amersham Biosciences). The blot was prehybridized at 68°C for 30 minutes and incubated with the radiolabeled probe at 68°C for 1 hour in the Expresshyb™ hybridization solution (Clontech). After hybridization, the blot was washed according to the Clontech Laboratories' protocol (manual PT1190-1). The blot was analyzed by autoradiography at –80°C using Kodak X-OMAT-AR X-ray film and an intensifying screen (1 day and 3 days of exposure). The blot was then stripped and, before a new hybridization, re-exposed for 3 days to ascertain the complete removal of the radioactive probe.

PCR screening of murine tissues

Multiple-tissue cDNA (MTC™) panel (Clontech, catalog number K1423-1) was used as source of first-strand cDNA for PCR amplification. Reactions were performed using either the sense primer S-TM5 (5′-TGTTCTGGTTCGGCATAGGGAAAGCCAC-3′) with the antisense primer AS-exon 26 (5′-CTTGTCATAAC-AGGATTGTGAACACC-3′) corresponding, respectively, to the beginning of the fifth transmembrane domain (nucleotides 2545-2572) and part of the cytoplasmic tail (nucleotides 2724-2749) of kidney-derived prominin-1.s1, or S-TM5 in conjunction with AS-T1. PCRs were carried out according to manufacturer's instructions using Advantage cDNA polymerase mix (Clontech) for 30 cycles of denaturation (94°C, 30 seconds), annealing (67°C, 30 seconds), extension (68°C, 1 minute) in a PTC-200 Peltier thermal cycler (MJ Research, Boston). Aliquots of the PCR products were resolved by electrophoresis in 1.5% agarose gel and stained with ethidium bromide.

Plasmid construction and transfection

The complete coding sequence of prominin-1.s3 splice variant was placed under the control of the CMV promoter by releasing the 2.8 kb *Hin*dIII-*Not*I fragment from the pCR-Blunt II-TOPO based

plasmid and ligating it into the eukaryotic expression vector pRc/CMV (Invitrogen) digested with the same restriction enzymes, thus generating pRc/CMV-s3. The constructs pRc/CMV-s4, pRc/CMV-s5 and pRc/CMV-s6 were generated by replacing the 2.4 kb *Xba*I fragment of pRc/CMV-s3 with the 2.3 kb, 2.3 kb and 2.6 kb *Xba*I-*Spe*I fragments from the s4-, s5- and s6-containing pCR-Blunt II-TOPO plasmids, respectively. All constructs were verified by sequencing.

CHO cells were cultured as described previously (Corbeil et al., 2000) and transfected at 50% confluence with the prominin-1 eukaryotic expression plasmids using Lipofectamine (Invitrogen) according to the supplier's instructions. Cells expressing the neomycin resistance gene were then selected by adding 600 μg ml^{-1} of G418 into the incubation medium. Ten days later, G418-resistant colonies were pooled and expanded. To enhance the expression of the transgene, cells were incubated for 17 hours with 5 mM sodium butyrate. Under these conditions, 10-30% of neomycin-resistant cells expressed recombinant prominin-1. Stably transfected CHO cells were then used for immunofluorescence and electron microscopy, or were solubilized in ice-cold solubilization buffer [1% Triton X-100, 0.1% sodium dodecyl sulfate (SDS), 150 mM NaCl, 5 mM EGTA, 50 mM Tris-HCl pH 7.5, 1 mM phenylmethylsulfonyl fluoride (PMSF), 2 μg ml^{-1} leupeptin, 10 μg ml^{-1} aprotinin] and detergent-cell extracts obtained after centrifugation (10 minutes, 10,000 ***g***, 4°C) were used for deglycosylation and immunoblotting.

Membrane preparations

Kidney, testis and epididymis from adult C57BL/6 mouse were homogenized in buffered sucrose (300 mM sucrose, 1 mM EDTA, 10 mM Hepes-KOH, pH 7.5, 1 mM PMSF, 2 μg ml^{-1} leupeptin, 10 μg ml^{-1} aprotinin, 100-200 mg tissue per 5 ml buffer) at 4°C using ten strokes in a glass-Teflon homogenizer at 3000 rpm, and centrifuged at 1000 ***g*** for 10 minutes. The supernatant was centrifuged at 40,000 ***g*** for 30 minutes, and the membrane pellet resuspended in 1% SDS, 20 mM sodium phosphate, pH 7.5, and boiled for 2 minutes.

Endoglycosidase digestion and immunoblotting

Proteins in the solubilized adult mouse membranes (40-80 μg protein) and in the CHO detergent-cell extracts corresponding to one-tenth of a 70% confluent 100-mm dish were incubated overnight at 37°C in the absence or presence of 1 unit peptide-N-glycosidase F (PNGase F) according to the manufacturer's instructions (Roche Molecular Biochemicals, Mannheim, Germany). Proteins were analyzed by SDS polyacrylamide-gel electrophoresis (SDS-PAGE) and transferred to poly(vinylidene difluoride) membranes (Millipore, Bedford, MA; pore size 0.45 μm) using a semi-dry transfer cell system (Cti, Idstein, Germany). After transfer, membranes were incubated for 30 minutes at room temperature in blocking buffer (PBS containing 5% low fat milk powder and 0.3% Tween 20). Prominin-1 splice variants were then detected using either rat monoclonal antibody (mAb) 13A4 (1 μg ml^{-1}) (Weigmann et al., 1997) or αI3 antiserum (1:20,000) (Corbeil et al., 1999) diluted in blocking buffer. Incubations of the primary antibodies were performed either overnight at 4°C in the case of mAb 13A4 or for 1 hour at room temperature in the case of αI3 antiserum. In both cases, antigen-antibody complexes were revealed using horseradish-peroxidase-conjugated secondary antibodies followed by enhanced chemiluminescence (ECL System, Amersham).

Immunofluorescence and confocal microscopy

Indirect immunofluorescence microscopy analysis of intact or paraformaldehyde-fixed Triton-X-100-permeabilized transfected CHO cells grown on glass coverslips were performed as described previously (Corbeil et al., 1999; Maw et al., 2000). For cell-surface immunofluorescence, the cells were double labeled at 4°C with mAb 13A4 (10 μg ml^{-1}) and fluorescein-isothiocyanate-conjugated wheat-germ agglutinin (WGA) (1:1200; Sigma) followed by Cy3-conjugated anti-rat secondary antibody (1:150; Dianova). In experiments with permeabilized cells, the WGA labeling was omitted. Cells were observed with a Leica SP2 confocal laser-scanning microscope. The confocal microscope settings were such that the photomultipliers were within their linear range. The images shown were prepared from the confocal data files using Adobe® Photoshop® software.

Immunohistochemistry of mouse tissues

Tissues were dissected from adult NMRI mice, embedded in Jung tissue-freezing medium (Leica), frozen on powdered dry ice and stored at –80°C. Cryosections (12 μm) were cut in a Leica Frigocut 2800N and mounted on slides coated with TESPA (triethoxysilylpropylamine) (Sigma). The sections were air-dried for several hours and fixed with 4% paraformaldehyde in PBS for 15 minutes at room temperature. The fixative was removed by two washes with PBS and residual formaldehyde was quenched with 50 mM NH_4Cl in PBS for 10 minutes. After two washes with PBS, sections were permeabilized with 0.3% saponin in PBS, washed and blocked in 5% fetal calf serum, 1% bovine serum albumin (BSA) in PBS (blocking solution) for 1 hour. The sections were then double labeled with mAb 13A4 (10 μg ml^{-1}) and αI3 antiserum (1:3000) in blocking solution overnight at 4°C. After washing, sections were incubated with secondary antibodies [Cy3-conjugated goat anti-rat IgG/IgM (1:150) and Cy2-conjugated goat anti-rabbit IgG/IgM (1:250); Dianova] diluted in blocking solution for 30 minutes at room temperature. Unbound antibodies were removed by several washes with PBS and nuclei were labeled with Hoechst 33258 (2 μg ml^{-1} in PBS, 5 minutes; Sigma). The sections were washed and mounted in Moviol 4.88 (Calbiochem). The samples were examined using a fluorescence microscope (Olympus BX61) and, for any given antibody, photographed with the same exposure time and printed in a standardized manner.

In experiments with immunoperoxidase, tissues dissected from adult C57Bl/6 mice were fixed by immersion in 4% paraformaldehyde in PBS overnight in 4°C. Tissues were infiltrated with cryoprotectant (30% sucrose in PBS), embedded in Tissue-Tek® (Miles, USA) and rapidly frozen on dry ice. Cryosections (12 μm) were mounted on SuperFrost®Plus (Menzel-Glaser, Germany) slides. Cells were permeabilized and sections blocked with 10% fetal calf serum and 0.2% saponin in PBS, and the endogenous peroxidase was neutralized with 1% H_2O_2 for 15 minutes. After washing, sections were incubated sequentially with mAb 13A4 (10 μg ml^{-1}) and peroxidase-coupled goat anti-rat antibody (1:300) (Dianova) for 1 hour at 37°C. Color reactions were performed with peroxidase substrate DAB (3,3′-diaminobenzidine tablet sets, 0.7 mg ml^{-1}; Sigma) according to the manufacturer's protocol. Stained sections were observed with an Olympus BX61 microscope.

Immunogold electron microscopy

CHO cells stably transfected with prominin-1.s3 and s6 variants cultured on collagen-coated Petri dishes (Collagen R; Serva) were washed with 200 mM Hepes-NaOH, pH 7.4, and fixed on the dish by addition of 4% paraformaldehyde in the same buffer at room temperature followed by incubation for 30 minutes at 4°C. The fixed cells were scraped off the dish and centrifuged (5 minutes, 200 ***g***), and the cell pellet incubated in fixative for another 3 hours. The cells were infiltrated with 2.1 M sucrose in PBS and frozen in liquid nitrogen. Epididymis of adult mice was fixed with 8% paraformaldehyde in 250 mM Hepes-NaOH, pH 7.4, for 3 hours at 4°C. Tissue pieces were then infiltrated with 15% polyvinylpyrrolidone, 1.95 M sucrose in PBS (Tokuyasu, 1989). Ultrathin cryosections were prepared as described previously (Corbeil et al., 1999; Maw et al., 2000). Immunogold labeling of cryosections using either rat mAb 13A4 (300 μg ml^{-1}) or

rabbit αE3 antiserum (1:50) (Maw et al., 2000), followed by rabbit anti-rat antibody (1:35) (Jackson ImmunoResearch Laboratories) and/or 15 nm colloidal-gold/protein-A was performed essentially as previously described (Corbeil et al., 1999). The sections were treated with 0.3% uranyl acetate/1.8% methylcellulose and air dried. Immunogold-labeled sections were examined with a Zeiss electron microscope (EM 10; Zeiss, Oberkochen, Germany).

Results

Identification and sequence analysis of novel splice variants of prominin-1

To identify novel splice variants of prominin-1 (Weigmann et al., 1997), databases were searched with mouse-kidney-derived prominin-1 (referred to as prominin-1.s1) (Fargeas et al., 2003b). Thereupon, the testis-derived EST clone 4932412G18 (which displayed a distinct, shorter cytoplasmic C-terminal domain) was used to amplify by PCR the entire open reading frame of the prominin-1 splice variant from a mouse testis cDNA pool. Four distinct alternatively spliced transcripts of prominin-1, named s3, s4, s5 and s6 were obtained (GenBank accession numbers AF305215, AY223521, AY223522 and AY099088). The predicted proteins deduced therefrom would contain 834, 804, 809 and 823 amino acids, respectively (Fig. 1A). Like the EST clone 4932412G18, s3, s4 and s5 variants contain a new cytoplasmic C-terminal domain (Fig. 1A, red letters) resulting from the use of an alternative splice acceptor site (AG) located within intron 24 [see supplementary Fig. S1B (http://jcs.biologists.org/cgi/content/full/117/18/4301/DC1)]. In addition, the s4 and s5 variants bore two and one in-frame deletion(s), respectively, in the extracellular domain(s) (Fig. 1A, amino acids in brackets). The 25 amino acid residues deleted from the second extracellular domain of the s4 and s5 variants correspond to those encoded by the entire exon 10 of the murine *prominin-1* gene (Fargeas et al., 2003a). The five amino acids deleted from the first extracellular domain of s4 variant result from the presence of an internal splice acceptor site (AG) within exon 5 (see supplementary Fig. S1A). The s6 variant retains the entire intron 24 (i.e. the 237-bp intervening sequence) (see supplementary Fig. S1B, bottom, black lowercase letters) between exon 24 (see supplementary Fig. S1B, blue letters) and the alternative splice acceptor site located within intron 24 (see supplementary Fig. S1B). The intron retention in the prominin-1.s6 transcript introduced a premature termination codon (TGA) and consequently generated a distinct, shorter C-terminal domain (Fig. 1A).

To determine the 3′-untranslated region (3′-UTR) of the novel prominin-1 splice variants, a 3′-RACE was performed using mouse 11-day whole-embryo cDNA pool. This source was used because the s3-s6 variants were detected therein (Fig. 2C). Two PCR products of 1653 bp and 1229 bp arose (see supplementary Fig. S1C). DNA sequencing showed that these PCR cDNA fragments, in addition to the testis-splice-variant-derived sequence identified above (see supplementary Fig. S1C, red letters), contained the remaining of the originally described intron 24 (see supplementary Fig. S1C, black capital letters) followed by the prominin-1.s1 cDNA nucleotide sequence (Weigmann et al., 1997) including exon 25-28 of murine *prominin-1* gene (see supplementary Fig. S1C, green and blue letters), which shows that prominin-1 variants do originate from the same transcription unit.

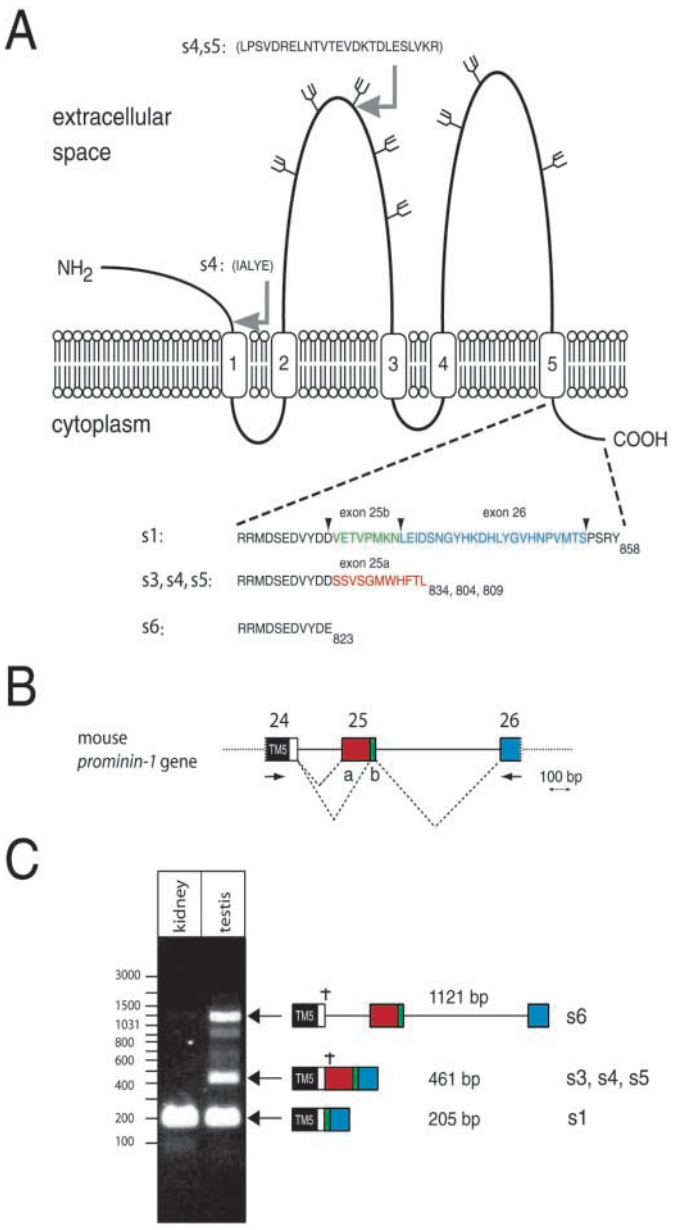

Fig. 1. Identification and characterization of multiple mouse prominin-1 splice variants. (A) Sites of alternative splicing in prominin-1. The C-terminal sequences of the testis-derived splice variants s3, s4, s5 and s6 are distinct from that of the previously described kidney-derived prominin-1.s1. Arrowheads indicate exon boundaries in the *prominin-1* gene. In addition, the s4 variant lacks five amino acid residues in the first extracellular domain, and the s4 and s5 variants both lack a facultative exon in the second extracellular domain (gray arrows, sequences in parentheses). Forks indicate the potential *N*-glycosylation sites. (B) Genomic organization of part of the murine *prominin-1* gene. Exons 24-26 appear as boxes and introns as solid lines. Exons 25a and 25b are in red and green, respectively. The position of the fifth transmembrane domain (TM5) is indicated in black. Arrows mark the position of the prominin-1-specific primers S-TM5 (left) and AS-exon 26 (right) used for PCR analysis. (C) Distinct *prominin-1* mRNAs are generated by the use of alternative acceptor sites (s3-s5) and by intron retention (s6). PCR reactions were performed using first-strand cDNA prepared from mouse kidney or testis as template, and the primers indicated in (B). Arrows indicate the three major PCR products and the corresponding prominin-1 mRNA species. †, the 3′ end of the open reading frame.

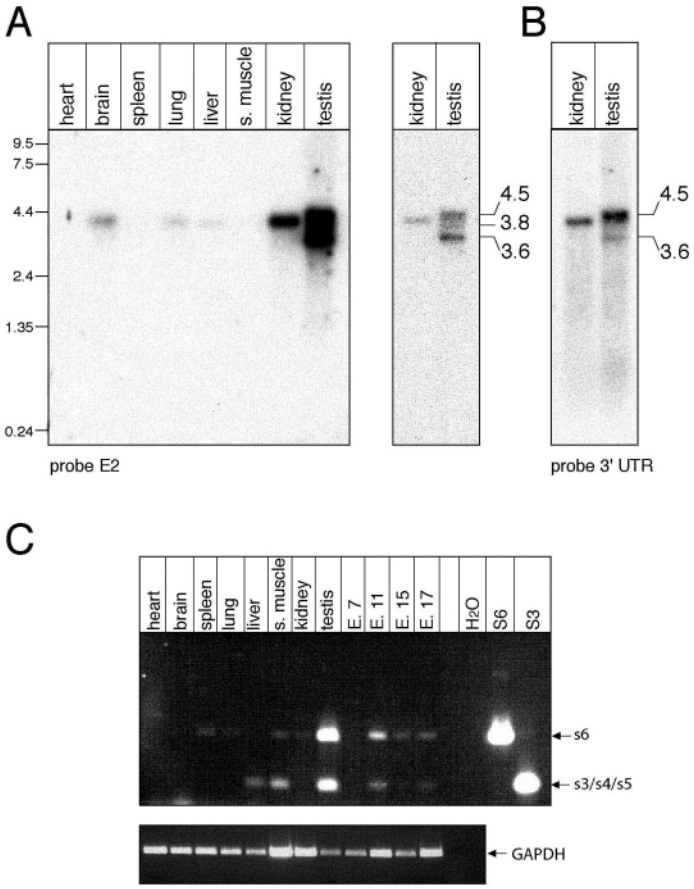

Fig. 2. Tissue distribution of mouse *prominin-1* splice variant mRNAs. (A,B) Northern blot of poly(A)$^+$ RNA (~2 μg each) from various mouse tissues, analyzed first with cDNA probe E2 (A) and then with a probe for the 3′-UTR (B). (A) The membrane was exposed for 1 day (right) and 3 days (left). (B) The membrane was exposed for 3 days. RNA size markers are indicated on the left (A). (C) PCR reactions were performed using first-strand cDNA prepared from mouse tissues as template using S-TM5 and AS-T1 primers located in exons 24 and 25a, respectively. Prominin-1.s3 and s6 variant cDNAs were used as templates for positive controls (lanes s3 and s6). As a negative control, template was omitted (lane H_2O). PCR for glyceraldehyde-3-phosphate dehydrogenase (GAPDH) expression was performed as a quality control. Embryonic stages (7- to 17-day-old embryos) are indicated as E7 to E17.

To document the expression of theses distinct cytoplasmic C-terminal domains, the use of an alternative acceptor splice site in the case of the s3-s5 variants and intron retention in the case of the s6 variant, we performed a reverse-transcription PCR (RT-PCR) using two specific primers flanking the testis-derived sequence (Fig. 1B, red box). Interestingly, although only a single major PCR product was amplified from a kidney cDNA pool, up to five PCR products were generated when a testis cDNA pool was used (Fig. 1C). Sequencing of the three major cDNA fragments amplified 205 bp, 461 bp and 1121 bp revealed that they corresponded to the s1, s3/s4/s5 and s6 variants, respectively. Thus, exon 25 of the murine *prominin-1* gene appears larger than initially thought (Fargeas et al., 2003a) with two alternative splice acceptor sites, a and b. In the case of the s1 variant, the distal (b) site is used, whereas, in the case of variants s3 to s5, the proximal (a) site is used. From now on, we use the terms exon 25a and 25b (Fig. 1A,B) [see supplementary Fig. S1C (http://jcs.biologists.org/cgi/content/full/117/18/4301/DC1)].

Expression of prominin-1 splice variant mRNAs in murine tissues

To determine the mRNA expression profile of the new prominin-1 splice variants, we performed northern-blot and RT-PCR analyses. The northern blot was probed using two distinct non-overlapping prominin-1 cDNA fragments of the mouse s1 variant corresponding either to a part of the coding region (probe E2) or to a 3′-UTR segment (probe 3′-UTR). Consistent with previous reports (Weigmann et al., 1997; Miraglia et al., 1998), probe E2 revealed a single 4.0-kb transcript in kidney, brain and lung (Fig. 2A, left). A faint band also appeared in liver (Fig. 2A, left). In testis, a strong, broad signal was detected (Fig. 2A, left) that, upon shorter exposure, appeared as three discrete transcripts of ~4.5 kb, 3.8 kb and 3.6 kb (Fig. 2A, right). Remarkably, two of these bands (4.5 kb and 3.6 kb) were also detected with the 3′-UTR probe (Fig. 2B), indicating that they contained the 3′-UTR of the s1 variant, in agreement with the results of 3′-RACE (see supplementary material, Fig. S1C).

To extend the northern blot analyses, we examined the expression pattern of the testis-derived splice variants (s3-s6) by RT-PCR, using an upstream primer corresponding to the sequence of the beginning of the fifth transmembrane domain (inside exon 24) and a downstream primer specific for the testis-expressed sequence (inside exon 25a). Although not strictly quantitative, this assay detected higher levels of prominin-1 splice variant mRNAs in testis than in the other tissues tested (Fig. 2C). Interestingly, the tissue distributions of the s3, s4, s5 and s6 variant mRNAs were distinct. The 455-bp PCR product corresponding to the s6 variant was detected in testis, skeletal muscle, kidney, lung and spleen, whereas the 218-bp PCR product corresponding to the s3, s4 and s5 variants was amplified from testis, skeletal muscle and liver. The expression of these prominin-1 variants also appears to be regulated during embryonic development, with an expression peak at day 11 (Fig. 2C).

Expression of prominin-1 splice variants in the adult murine epididymis and testis

Next, we investigated the actual protein expression of the novel prominin-1 splice variants by immunoblotting. We used two antibodies, the rat mAb 13A4 (Weigmann et al., 1997), which recognizes an epitope localized in the second extracellular loop of prominin-1 (Maw et al., 2000), and the rabbit antiserum αI3 directed against the cytoplasmic C-terminal domain of the s1 variant (Corbeil et al., 1999). The latter should fail to detect any of the newly identified prominin-1 splice variants.

Immunoblotting of membrane lysates from the testis and epididymis using mAb 13A4 revealed a broad band with an apparent molecular mass of 100-112 kDa (Fig. 3A, control, lane T and E), which was slightly smaller than that detected in kidney membranes (~115 kDa) (Fig. 3A, control, lane K). Interestingly, when the testis and epididymis were separated from each other, the testis was found to contain a sharp band

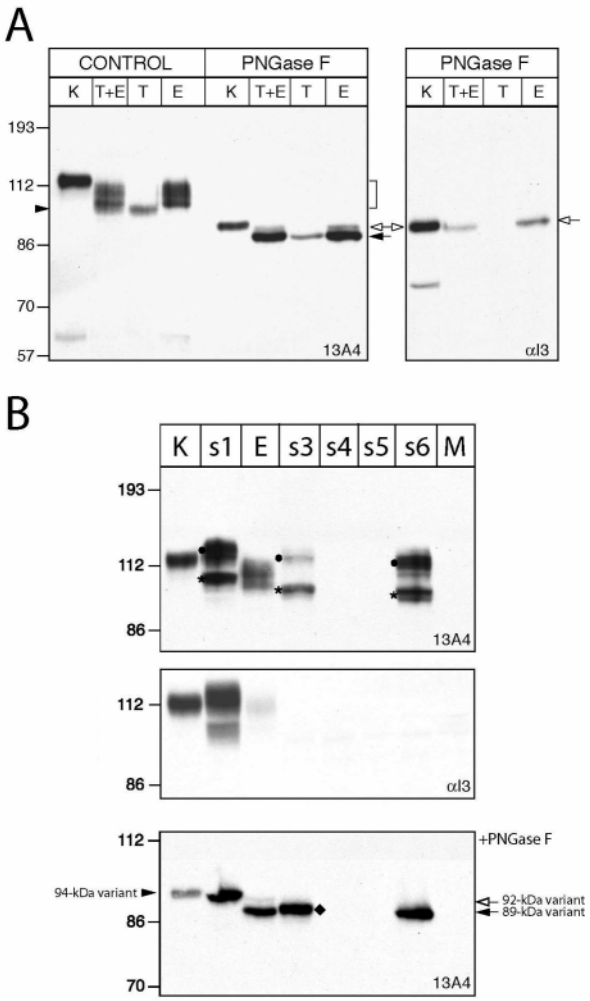

Fig. 3. Characterization of prominin-1 splice variants in the adult murine male reproductive system. (A) Proteins solubilized from adult mouse testis and epididymis membranes (T+E, 80 μg protein), testis membranes (T, 80 μg protein) and epididymis membranes (E, 40 μg protein) were incubated in the absence (CONTROL) or presence (PNGase F) of PNGase F, and analyzed by immunoblotting using either mAb 13A4 (13A4, left) or αI3 antiserum (αI3, right). For comparison, prominin-1 from adult kidney membranes (K, 50 μg protein) was analyzed in parallel. Arrowhead, glycosylated 100-kDa form of testis-derived prominin-1; bracket, glycosylated 104-112 kDa forms of epididymis-derived prominin-1; open arrows, *N*-deglycosylated, 13A4- and αI3-immunoreactive 92-kDa form of epididymis-derived prominin-1; solid arrow, *N*-deglycosylated, 13A4-immunoreactive, αI3-nonreactive 89-kDa form of testis/epididymis-derived prominin-1. (B) Lysates prepared from CHO cells transfected with prominin-1 splice variants s1, s3, s4, s5 or s6, or with vector DNA without insert (M), and, for comparison, prominin-1 from adult kidney (K) and epididymis (E) membranes, were incubated in the absence (top, middle) or presence (bottom) of PNGase F and analyzed by immunoblotting. (Top) Asterisks, endo-H-sensitive forms of recombinant prominin-1; dots, endo-H-resistant forms of recombinant prominin-1. (Bottom) Arrowhead, *N*-deglycosylated 94-kDa form of kidney-derived prominin-1; open arrow, *N*-deglycosylated 92-kDa form of epididymis-derived prominin-1; solid arrows, *N*-deglycosylated 89-kDa form of epididymis-derived prominin-1; diamond, *N*-deglycosylated 90-kDa form of recombinant s3 variant. Notice that the 89-kDa form of epididymis-derived prominin-1 and recombinant s6 variant exhibit an indistinguishable electrophoretic mobility upon *N*-deglycosylation, whereas the recombinant s3 variant shows a slightly lower electrophoretic mobility (90 kDa).

of ~100 kDa (Fig. 3A, control, lane T, arrowhead), whereas the epididymis contained bands of more heterogeneous electrophoretic mobility (104-112 kDa) (Fig. 3A, control, lane E, bracket). This suggests a possibly tissue-specific glycosylation process and/or the expression of distinct prominin-1 splice variants in these tissues. To investigate this issue, membrane extracts were incubated with PNGase F before analysis. Upon removal of N-linked glycans, two distinct prominin-1 immunoreactive bands of ~92 kDa and ~89 kDa were observed in the epididymis when mAb 13A4 was used (Fig. 3A, left, PNGase F, lanes T+E and E, white and black arrows). Only one, the ~92 kDa band, was detected with the αI3 antiserum (Fig. 3A, right, lanes T+E and E, white arrow). This suggests that the 89 kDa band, which was the major band in epididymis, represents a splice variant of prominin-1 lacking the C-terminal domain of the s1 variant expressed in kidney (Fig. 3A, right, lane K) (see also Weigmann et al., 1997). The 89 kDa band was also detected in testis, although its expression level was very low compared with that in epididymis (Fig. 3A, left, PNGase F, lane T, black arrow). Together, these data show that a specific splice variant of prominin-1 containing a distinct C-terminal domain is expressed in the male reproductive system, mainly in the epididymis. Moreover, the observations that both epididymis and testis yielded the same 89 kDa product after deglycosylation even though the glycosylated proteins had distinct apparent molecular masses implies that the glycosylation of this splice variant differs between the epididymis and testis.

Heterologous expression of prominin-1 splice variants in CHO cells

To characterize further the different prominin-1 splice variants, CHO cells were stably transfected with the corresponding cDNAs and analyzed by immunoblotting (Fig. 3B). Recombinant s1, s3 and s6 variants each displayed two 13A4-immunoreactive bands with apparent molecular masses of ~110/115 kDa and ~100/104 kDa (Fig. 3B, top), whereas CHO cells transfected with s4 or s5 variants, or, as negative control, vector alone did not show any immunoreactivity (Fig. 3B, top). The ~100/104 kDa forms of recombinant s1, s3 and s6 variants (Fig. 3B, top, asterisks) were sensitive to digestion with endo H (data not shown) and therefore represented the high-mannose form localized to the endoplasmic reticulum (ER) and/or an early Golgi compartment. The ~110/115 kDa forms (Fig. 3B, top, circles) were resistant to endo H (data not shown), indicating that they had passed through the Golgi

apparatus. As expected, recombinant s3 and s6 were not detected with αI3 antiserum (Fig. 3B, middle, lanes s3 and s6).

To determine which splice variants of prominin-1 are expressed in the testis and epididymis, membrane extracts derived from kidney and epididymis were analyzed in parallel with individual recombinant prominin-1 splice variants (Fig. 3B, lanes K and E). After PNGase-F treatment, the deglycosylated recombinant s6 variant exhibited an electrophoretic mobility indistinguishable from that of the major 89 kDa band detected in epididymis (Fig. 3B, bottom, lanes E and s6, black arrow). By contrast, the deglycosylated recombinant s3 variant reproducibly showed a slightly slower electrophoretic mobility (90 kDa) than the 89 kDa band from epididymis. These data are consistent with the notion that the major prominin-1 splice variant protein expressed in the adult male reproductive system is s6.

None of the deglycosylated recombinant s3 and s6 splice variants showed an electrophoretic mobility similar to that of the minor 92 kDa band observed in epididymis (Fig. 3B, bottom, lane E, open arrow). This minor band, which will be referred to as the 92-kDa variant, appears to be slightly smaller than the kidney-derived prominin-1.s1 variant (94 kDa) but, in contrast to the s6 variant, still exhibits αI3 immunoreactivity (Fig. 3A,B). It thus might constitute an additional, s1-related prominin-1 splice variant.

Cell-surface expression and localization to plasma-membrane protrusions of s3 and s6 in non-epithelial cells

To determine whether the prominin-1 splice variants reach the plasma membrane, cell-surface immunofluorescence with mAb 13A4 followed by confocal laser-scanning microscopy was performed on CHO cells stably transfected with s1, s3, s4, s5 and s6 variants. To facilitate the analysis, the CHO cell surface was visualized with WGA (green) staining. Analysis of single optical sections across the middle of the cells showed that the s3 and s6 variants (red), but not the s4 and s5 variants, were expressed on the cell surface (Fig. 4A) like the s1 variant (Fig. 4A, inset). When paraformaldehyde-fixed prominin-1.s4 and s5-transfected CHO cells were permeabilized with Triton X-100, only a weak intracellular staining characteristic for the ER was observed (Fig. 4B). Together with the lack of immunoreactive bands observed by immunoblotting (Fig. 3B, lanes s4 and s5), this suggests that s4 and s5 variants do not traffic out the ER and are presumably subject to ER degradation.

The remarkable feature of prominin-1 [its specific localization to microvillar membranes and other plasma-membrane protrusions in various cell types (Weigmann et al., 1997; Corbeil et al., 2001b)] prompted us to investigate the subcellular localization of s3 and s6 variants in transfected CHO cells. Immunogold electron microscopy performed with either mAb 13A4 or the rabbit antiserum αE3 directed against the second extracellular loop of the s1 variant (Maw et al., 2000) revealed that, for both splice variants, immunoreactivity was preferentially associated with small plasma-membrane protrusions, whereas large, neighboring planar surfaces of the plasma membrane were much more weakly labeled (Fig. 4C). In line with our previous data (Corbeil et al., 1999), it thus appears that the truncation of the cytoplasmic C-terminal domain of the s1 variant or its substitution by a new peptide sequence encoded by exon 25a in the case of s3 does not interfere with intracellular trafficking or the concentration of these molecules in plasma-membrane protrusions.

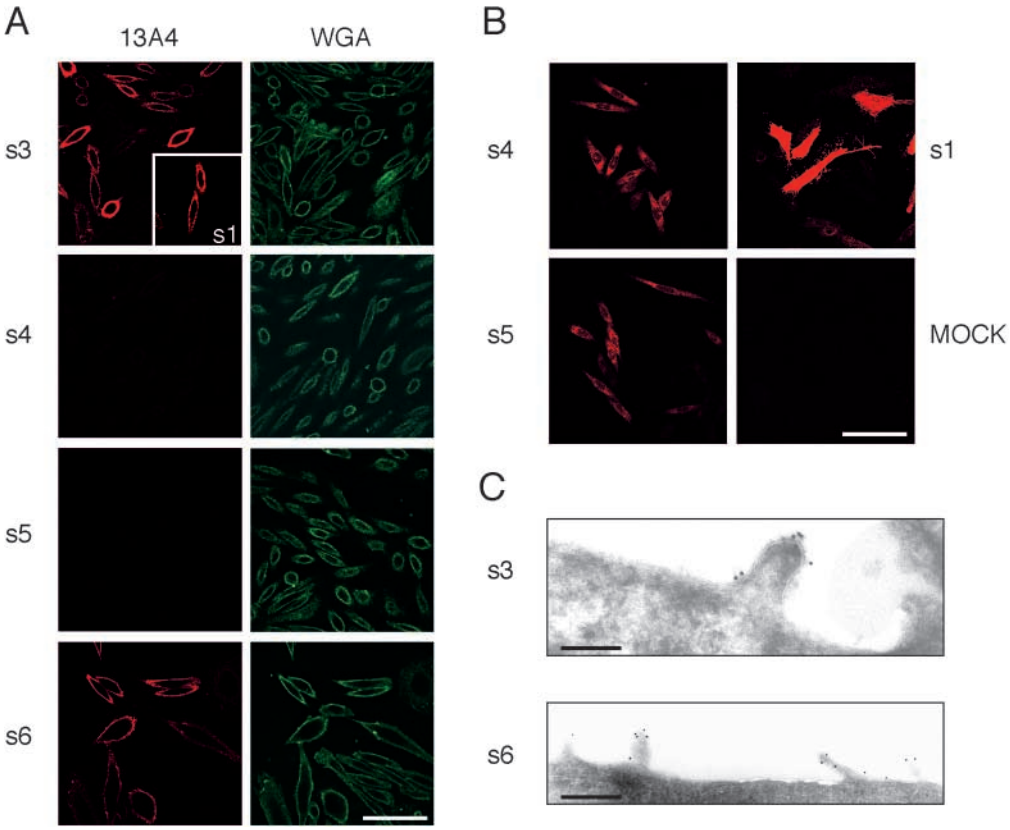

Fig. 4. Cell surface expression and localization in plasma-membrane protrusions of prominin-1.s3 and s6 splice variants in CHO cells. (A,B) CHO cells stably transfected with prominin-1 splice variants s1 (positive control), s3, s4, s5, s6 or with vector DNA without insert (MOCK) were either double cell-surface labeled with the mAb 13A4 and FITC-conjugated wheat-germ agglutinin (WGA) (green) followed by Cy3-conjugated anti-rat secondary antibody (red) (13A4) (A) or labeled after paraformaldehyde fixation and Triton-X-100 permeabilization with mAb 13A4 followed by Cy3-conjugated anti-rat secondary antibody (red) (B). (A) Single optical sections at the level of the middle of the cells. (B) Composite pictures of eight optical sections. Scale bars, 45 μm (A), 60 μm (B). (C) Ultrathin cryosections of CHO cells transfected with s3 and s6 splice variants were stained with either the mAb 13A4 (s3) or αE3 antiserum (s6) followed by rabbit anti-rat IgG/IgM and/or 15-nm Protein-A/gold. Scale bars, 245 nm (s3); 420 nm (s6).

Localization of prominin-1 in the murine epididymis and testis

Given the high expression of prominin-1 in adult mouse epididymis, it was interesting to investigate its distribution by immunohistochemistry. A strong staining with both mAb 13A4 and αI3 antiserum was detected at the apical side of the epithelial cells lining the ductuli efferentes (Fig. 5B). In the epididymis proper, the initial segment of the head, where the ductuli efferentes end (Fig. 5A), was devoid of prominin-1 immunoreactivity (Fig. 5B). By contrast, the proximal (data not shown) and distal (Fig. 5B) parts of the caput (head) displayed prominin-1 immunoreactivity with both antibodies. As for ductuli efferentes, immunoreactivity was confined to the apical side of the epithelia. Remarkably, the corpus (body) exhibited 13A4, but not αI3, immunoreactivity, suggesting that this region expresses only the prominin-1 splice variant lacking the αI3 epitope (Fig. 5B). By contrast, the epithelium of the cauda (tail) was labeled with both antibodies (Fig. 5C). Although the αI3 immunoreactivity is weaker than the 13A4 immunoreactivity, the staining patterns superimpose irrespective of the epididymis region, except for the corpus (Fig. 5C, merge, and data not shown).

However, it is interesting that not all cells were stained (Fig. 5C, arrows). At the higher magnification, we saw that several cells of the cauda epithelium (Fig. 5D, boxes) and the epithelia of the corpus and caput (data not shown) were prominin-1 negative. This discontinuous expression pattern is reminiscent of that described for the water channel protein aquaporin 9, which is expressed only by principal and not by clear cells (Pastor-Soler et al., 2001).

With regard to the testis, we found that the 13A4, but not αI3, immunoreactivity was selectively associated with the tail of spermatozoa present in seminiferous tubules (Fig. 6A,B; data not shown) [see supplementary Fig. S2A (http://jcs.biologists.org/cgi/content/full/117/18/4301/DC1)]. Interestingly, once released into the epididymis, the spermatozoa no longer showed prominin-1 immunoreactivity (Fig. 5, asterisks, Fig. 6C). No prominin-1 immunoreactivity was detected in spermatogonia, spermatocytes and spermatids [see supplementary Fig. S2A), nor in Sertoli or Leydig cells (Fig. 6A,B).

Concentration of prominin-1 in the stereocilia of the epididymis

The subcellular localization of prominin-1 in the murine epididymis was investigated by immunogold electron microscopy using either mAb 13A4 (data not shown) or the

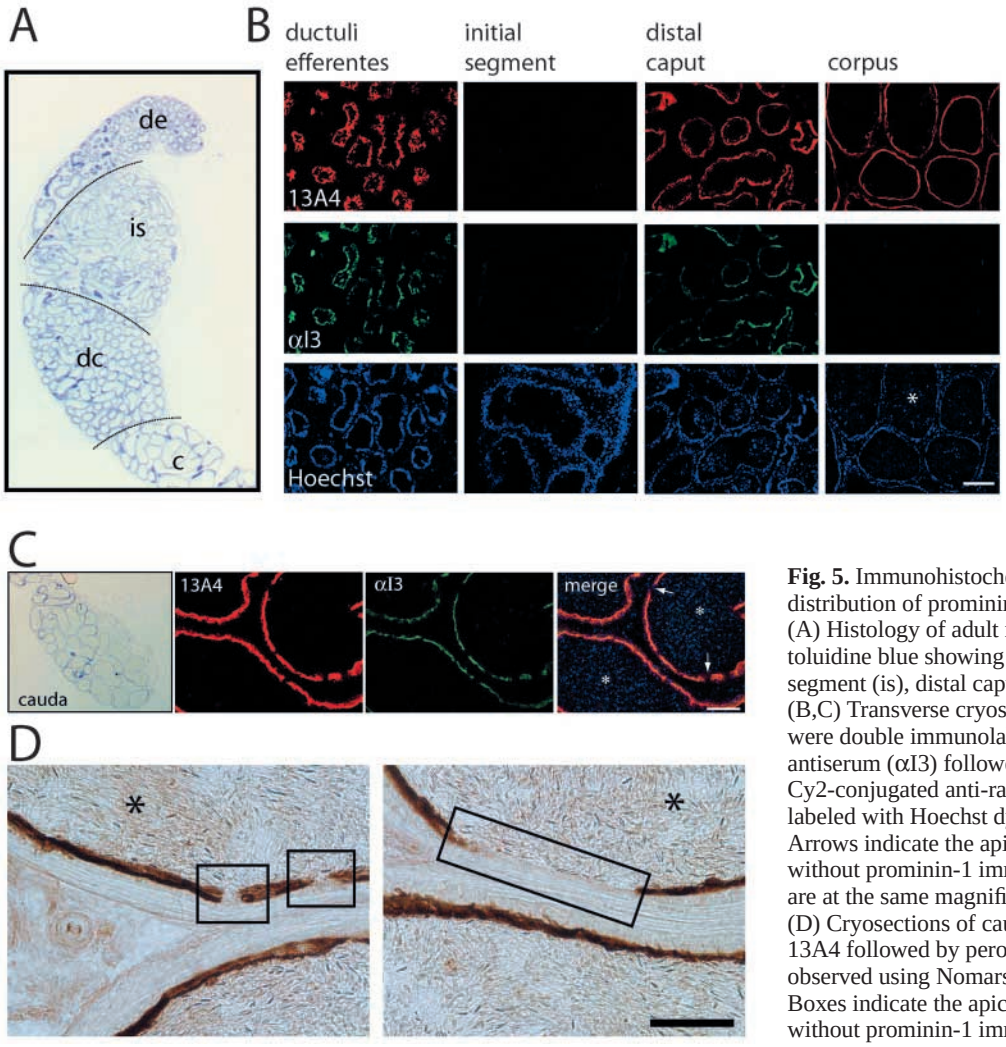

Fig. 5. Immunohistochemistry showing the regional distribution of prominin-1 in murine epididymis. (A) Histology of adult murine epididymis stained with toluidine blue showing the ductuli efferentes (de), initial segment (is), distal caput (dc) and part of the corpus (c). (B,C) Transverse cryosections of adult murine epididymis were double immunolabeled with mAb 13A4 (13A4) and αI3 antiserum (αI3) followed by Cy3-conjugated anti-rat and Cy2-conjugated anti-rabbit secondary antibodies. Nuclei were labeled with Hoechst dye. Asterisks mark spermatozoa. Arrows indicate the apical surface of the cauda epithelium without prominin-1 immunostaining. All fluorescence images are at the same magnification. Scale bars, 100 μm. (D) Cryosections of cauda were immunolabeled with mAb 13A4 followed by peroxidase-coupled goat anti-rat, and observed using Nomarski optics. Asterisks mark spermatozoa. Boxes indicate the apical surface of the cauda epithelium without prominin-1 immunostaining. Scale bar, 40 μm.

rabbit antiserum αE3 (Fig. 7). Strong labeling for the prominin-1 was observed on the microvilli/stereocilia of the apical surface of principal cells lining the duct of the corpus (Fig. 7A). As observed with non-epithelial cells (see above), the αE3 immunoreactivity was not detected in the non-protruding regions of the plasma membrane (Fig. 7A, arrows). Similar data were obtained with mAb 13A4 (data not shown). No specific immunoreactivity was detected when the primary antibody was omitted (Fig. 7B).

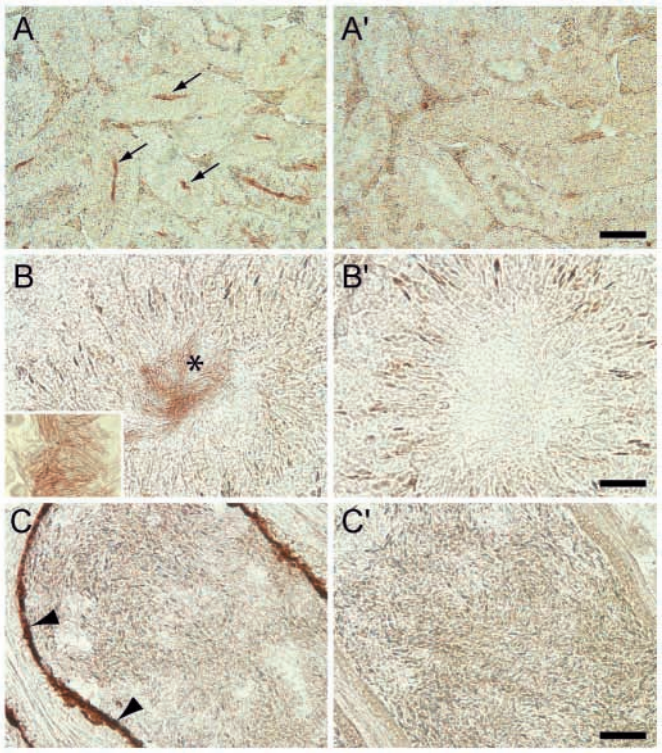

Fig. 6. Immunoperoxidase localization of prominin-1 in the tail of spermatozoa found in seminiferous tubules. Cryosections of adult murine testis (A,B) and epididymis (C) were immunolabeled with (A-C) or without (A′-C′) mAb 13A4 followed by peroxidase-coupled goat anti-rat, and observed using Nomarski optics. (A) Arrows indicate the lumen of seminiferous tubules. (B) The asterisk indicates the tail of spermatozoa, shown at high magnification in the inset. (C) Arrowheads indicate the apical surface of the corpus epithelium. Scale bars, 170 μm (A,A′); 30 μm (B,B′); 40 μm (C,C′).

Discussion

Our knowledge of the prominin family (Fargeas et al., 2003a; Fargeas et al., 2003b) is growing rapidly, because prominin-1 appears to be an important hematopoietic and neural stem cell marker. This five-membrane-span glycoprotein might well become an established tool not only for medical diagnosis but also for therapy. Therefore, a complete catalog of the different members of the prominin family, including splice variants and their tissue distribution and subcellular localization, is needed. Here, we have characterized several novel prominin-1 splice variants that contain distinct cytoplasmic C-terminal domains. These splice variants are expressed physiologically, in a tissue-specific manner and are developmentally regulated (Figs 1, 2).

This study provides biochemical and morphological evidence that, in the murine male reproductive system, specific prominin-1 splice variants show a distinct pattern of expression along the epididymal duct. Our biochemical data reveal that the 89-kDa prominin-1.s6 variant is predominantly expressed in the epididymis and in the testis, whereas the 92-kDa variant is found, at lower levels than the s6 variant, only in the epididymis. Moreover, the broad prominin-1-immunoreactive band observed by immunoblotting in epididymis (Fig. 3) suggests that a given individual splice variant, such as the s6 variant in epididymis, can exist in several distinct glycoforms. Likewise, the prominin-1 immunoreactivity observed in the testis displays a distinct pattern of glycosylation. The physiological significance of these prominin-1 glycoforms needs to be elucidated but such different *N*-glycan modifications in the male genital tract have been previously reported for other antigens [e.g. the CAMPATH-1 antigen (CD52) (Schroter et al., 1999)].

The epididymal duct is characterized by distinct regional zones that play a central role in the transport, maturation and concentration of sperm. The molecular basis for these functions is poorly understood, but the regional differences along the duct have been related not only to variations in cell morphology but also to distinct temporal and spatial expression of certain genes, with discrete regulatory mechanisms (Kirchhoff, 1999). Our combined biochemical and histological data show that prominin-1 splice variants display a specific regional expression [e.g. the lack of αI3 immunoreactivity in the corpus is consistent with the expression of 89-kDa s6 variant but not the 92-kDa variant in this specific region (Fig. 5B)]. The absence of either 13A4 or αI3 immunoreactivity in the initial segment might reflect the differential susceptibility

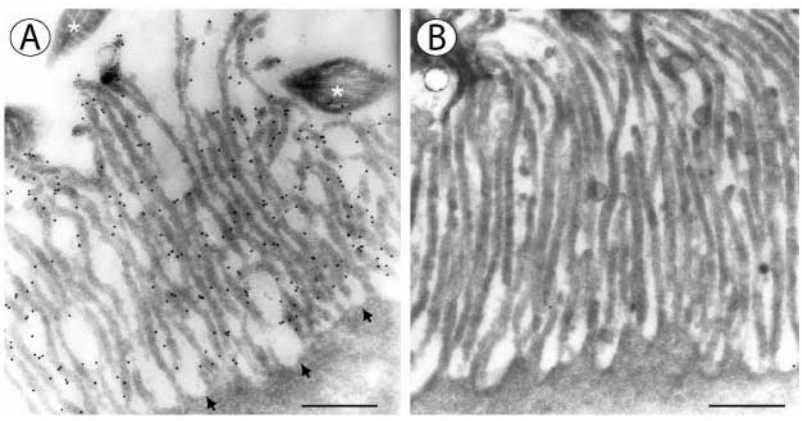

Fig. 7. Immunogold electron microscopy showing the subcellular localization of prominin-1 in murine epididymis. Ultrathin cryosections of the apical surface of epithelial cells lining the corpus of the epididymis were incubated with (A) or without (B) αE3 antiserum followed by 15-nm Protein-A/gold. Arrows indicate regions of the plasma membrane between the stereocilia; asterisks indicate spermatozoa. Scale bars, 625 nm (A); 640 nm (B).

of this section to circulating hormones and testicular factors compared with more distal segments of the epididymis (Brooks, 1983; Hess, 2003; Ezer et al., 2003), although evidence that prominin-1 expression is hormonally regulated is currently lacking. Yet, given the propensity of prominin-1 to undergo alternative splicing, the expression of an uncharacterized splice variant in this segment cannot be not formally excluded.

Regarding the subcellular localization of prominin-1 to the epididymis and testis, three key observations have been made. First, prominin-1 is confined to the apical microvilli/stereocilia of principal cells. Second, prominin-1 is concentrated in the tail of spermatozoa when present in the seminiferous tubules. Third, spermatozoa found in the epididymis no longer contain prominin-1. These data are consistent with the postulated function of prominin-1 as an organizer of the plasma-membrane protrusions and suggest that prominin-1 is involved in the formation and/or stabilization of epididymal stereocilia as well as the tails of spermatozoa. The discontinuous staining observed (particularly in the cauda segment) is consistent with the absence of prominin-1 in clear cells that have less-extensive microvilli than principal cells (Hamilton et al., 1977) is also in line with our findings. Thus, prominin-1 in the male reproductive system might play a dual role in the formation of spermatozoa and in their maturation, which occurs during their transit through the epididymal duct. Clearly, further studies are needed to clarify the role of prominin-1 in these processes, which are highly relevant for male fertility.

Aside from the presently characterized splice variants, mouse prominin-1.s7 and s8 variants have been reported in the database as full-length EST clones (GenBank accession numbers AK029921 and BC028286) (Fargeas et al., 2003b), and rat prominin-1.s7 cDNA has been isolated in our laboratory (GenBank accession number AY262731). Recently, the human prominin-1.s7 variant sequence has been deposited in database (GenBank accession number AY449690). In these variants, exons 25 (a and b) and 26 are skipped, resulting in the in-frame deletion of residues 824-854 of the s1 variant [see supplementary Fig. S3 (http://jcs.biologists.org/cgi/content/full/117/18/4301/DC1)].

The membrane-proximal portion of the cytoplasmic C-terminal tail of prominin-1 appears to be an important site of regulation, because different forms of alternative splicing occur at the corresponding site of the transcript (i.e. the 3′ boundary of exon 24), with: (1) intron retention (in the case of s6 variant); (2) extension of exon 25 by use of a cryptic acceptor site within intron 24 (s3, s4 and s5 variants); and (3) exon skipping (s7 and s8 variants). Moreover, this splicing cassette appears to be conserved across species, because exons corresponding to exon 25a are present in other mammalian [see supplementary Fig. S3 and lower-vertebrate *prominin* genes (e.g. GenBank accession numbers CA368604 and AC113578), further supporting the biological significance of this regulation. Our data show that the s3 and s6 variants are targeted to and concentrated in plasma-membrane protrusions in non-epithelial and epithelial cells, as previously reported for the s1 variant (Weigmann et al., 1997). Thus, the presence of alternative residues in the C-terminal domain does not interfere with intracellular trafficking or the retention in microvilli.

Another site of alternative splicing resides at the 3′ boundary of exon 3, because this can be spliced to exon 4 (s2 variant) (Miraglia et al., 1998; Yu et al., 2002), exon 5 (s1 variant) (Weigmann et al., 1997) or an internal acceptor site within exon 5 (s4 variant) (present study). Compared with the s2 variant, the consequence of the latter two splicing events is the deletion of 9 and 14 amino acids, respectively, from the N-terminal extracellular domain close to the first transmembrane domain. Such deletions do not seem to affect the cell-surface expression of the splice variants (Weigmann et al., 1997; Yu et al., 2002). The biological significance of the exon-10 skipping is currently more difficult to evaluate. It results in the in-frame deletion of 25 amino acid residues from the second extracellular domain, and the splice variants s4 and s5, which carry this deletion, failed to reach the cell surface upon transfection in CHO cells. They appear to be subject to ER degradation, probably because of improper folding of the first extracellular loop of the molecule. The intracellular environment provided by this specific cell line might be too different from the in vivo situation to allow correct folding unless such misfolding is intrinsic to the s4 and s5 molecules.

Further investigations are necessary to determine the biological significance of the splice variants described here, but the observations that prominin-1 undergoes tissue-specific alternative splicing might be relevant for human pathology, such as the case of retinal degeneration associated with a frame-shift mutation in the human *PROMININ-1* gene (Maw et al., 2000). Because the second large loop is encoded by a series of short, symmetric exons, the mutated exon (i.e. exon 16), which carries the single-nucleotide deletion (nucleotide 1878), could be skipped, resulting in a shorter loop but maintaining the five-membrane-span structure of prominin-1 in tissues other than retina. This might explain the lack of other obvious pathological symptoms in the affected individuals (Maw et al., 2000).

We thank R. Jelinek for valuable technical assistance and G. Wiebe for the excellent sequencing service. W.B.H. was supported by grants from the DFG (Hu 275/7, Hu 275/8), the German-Israeli Foundation for Scientific Research and Development, and the Fonds der Chemischen Industrie. Sequence data from this article have been deposited with the Database library under GenBank accession numbers AF305215, AY223521, AY223522, AY099088 and AY262731.

References

Bhatia, M. (2001). AC133 expression in human stem cells. *Leukemia* **15**, 1685-1688.

Boesze-Battaglia, K., Hennessey, T. and Albert, A. D. (1989). Cholesterol heterogeneity in bovine rod outer segment disk membranes. *J. Biol. Chem.* **264**, 8151-8155.

Brooks, D. E. (1983). Epididymal functions and their hormonal regulation. *Aust. J. Biol. Sci.* **36**, 205-221.

Corbeil, D., Röper, K., Weigmann, A. and Huttner, W. B. (1998). AC133 hematopoietic stem cell antigen – human homologue of mouse kidney prominin or distinct member of a novel protein family. *Blood* **91**, 2625-2626.

Corbeil, D., Röper, K., Hannah, M. J., Hellwig, A. and Huttner, W. B. (1999). Selective localization of the polytopic membrane protein prominin in microvilli of epithelial cells – a combination of apical sorting and retention in plasma membrane protrusions. *J. Cell Sci.* **112**, 1023-1033.

Corbeil, D., Röper, K., Hellwig, A., Tavian, M., Miraglia, S., Watt, S. M., Simmons, P. J., Peault, B., Buck, D. W. and Huttner, W. B. (2000). The human AC133 hematopoietic stem cell antigen is also expressed in epithelial cells and targeted to plasma membrane protrusions. *J. Biol. Chem.* **275**, 5512-5520.

Corbeil, D., Fargeas, C. A. and Huttner, W. B. (2001a). Rat prominin, like

its mouse and human orthologues, is a pentaspan membrane glycoprotein. *Biochem. Biophys. Res. Commun.* **285**, 939-944.

Corbeil, D., Röper, K., Fargeas, C. A., Joester, A. and Huttner, W. B. (2001b). Prominin: a story of cholesterol, plasma membrane protrusions and human pathology. *Traffic* **2**, 82-91.

Ezer, N. and Robaire, B. (2003). Gene expression is differentially regulated in the epididymis after orchidectomy. *Endocrinology* **144**, 975-988.

Fargeas, C. A., Florek, M., Huttner, W. B. and Corbeil, D. (2003a). Characterization of prominin-2, a new member of the prominin family of pentaspan membrane glycoproteins. *J. Biol. Chem.* **278**, 8586-8596.

Fargeas, C. A., Corbeil, D. and Huttner, W. B. (2003b). AC133 antigen, CD133, prominin-1, prominin-2, etc.: prominin family gene products in need of a rational nomenclature. *Stem Cells* **21**, 506-508.

Hamilton, D. W., Olson, G. E. and Cooper, T. G. (1977). Regional variation in the surface morphology of the epithelium of the rat ductuli efferentes, ductus epididymidis and vas deferens. *Anat. Rec.* **188**, 13-27.

Hess, R. A. (2003). Estrogen in the adult male reproductive tract: a review. *Reprod. Biol. Endocrinol.* **1**, 52.

Kirchhoff, C. (1999). Gene expression in the epididymis. *Int. Rev. Cytol.* **188**, 133-202.

Maw, M. A., Corbeil, D., Koch, J., Hellwig, A., Wilson-Wheeler, J. C., Bridges, R. J., Kumaramanickavel, G., John, S., Nancarrow, D., Röper, K. et al. (2000). A frameshift mutation in prominin (mouse)-like 1 causes human retinal degeneration. *Hum. Mol. Genet.* **9**, 27-34.

Miraglia, S., Godfrey, W., Yin, A. H., Atkins, K., Warnke, R., Holden, J. T., Bray, R. A., Waller, E. K. and Buck, D. W. (1997). A novel five-transmembrane hematopoietic stem cell antigen: isolation, characterization, and molecular cloning. *Blood* **90**, 5013-5021.

Miraglia, S., Godfrey, W. and Buck, D. (1998). A response to AC133 hematopoietic stem cell antigen: human homologue of mouse kidney prominin or distinct member of a novel protein family? *Blood* **91**, 4390-4391.

Pastor-Soler, N., Bagnis, C., Sabolic, I., Tyszkowski, R., McKee, M., van Hoek, A., Breton, S. and Brown, D. (2001). Aquaporin 9 expression along the male reproductive tract. *Biol. Reprod.* **65**, 384-393.

Röper, K., Corbeil, D. and Huttner, W. B. (2000). Retention of prominin in microvilli reveals distinct cholesterol-based lipid micro-domains in the apical plasma membrane. *Nat. Cell Biol.* **2**, 582-592.

Schroter, S., Derr, P., Conradt, H. S., Nimtz, M., Hale, G. and Kirchhoff, C. (1999). Male-specific modification of human CD52. *J. Biol. Chem.* **274**, 29862-29873.

Steinberg, R. H., Fisher, S. K. and Anderson, D. H. (1980). Disc morphogenesis in vertebrate photoreceptors. *J. Comp. Neurol.* **190**, 501-508.

Tokuyasu, K. T. (1989). Use of poly(vinylpyrrolidone) and poly(vinyl alcohol) for cryoultramicrotomy. *Histochem. J.* **21**, 163-171.

Uchida, N., Buck, D. W., He, D., Reitsma, M. J., Masek, M., Phan, T. V., Tsukamoto, A. S., Gage, F. H. and Weissman, I. L. (2000). Direct isolation of human central nervous system stem cells. *Proc. Natl. Acad. Sci. USA* **97**, 14720-14725.

Weigmann, A., Corbeil, D., Hellwig, A. and Huttner, W. B. (1997). Prominin, a novel microvilli-specific polytopic membrane protein of the apical surface of epithelial cells, is targeted to plasmalemmal protrusions of non-epithelial cells. *Proc. Natl. Acad. Sci. USA* **94**, 12425-12430.

Yin, A. H., Miraglia, S., Zanjani, E. D., Almeida-Porada, G., Ogawa, M., Leary, A. G., Olweus, J., Kearney, J. and Buck, D. W. (1997). AC133, a novel marker for human hematopoietic stem and progenitor cells. *Blood* **90**, 5002-5012.

Yu, Y., Flint, A., Dvorin, E. L. and Bischoff, J. (2002). AC133-2, a novel isoform of human AC133 stem cell antigen. *J. Biol. Chem.* **277**, 20711-20716.